NANO LETTERS

2006
Vol. 6, No. 11
2442−2446

Giant Enhancement of the Carrier Mobility in Silicon Nanowires with Diamond Coating

Vladimir A. Fonoberov and Alexander A. Balandin*

Nano-Device Laboratory, Department of Electrical Engineering, University of California—Riverside, Riverside, California 92521

Received July 6, 2006; Revised Manuscript Received September 15, 2006

ABSTRACT

We show theoretically that the low-field carrier mobility in silicon nanowires can be greatly enhanced by embedding the nanowires within a hard material such as diamond. The electron mobility in the cylindrical silicon nanowires with 4-nm diameter, which are coated with diamond, is 2 orders of magnitude higher at 10 K and a factor of 2 higher at room temperature than the mobility in a free-standing silicon nanowire. The importance of this result for the downscaled architectures and possible silicon–carbon nanoelectronic devices is augmented by an extra benefit of diamond, a superior heat conductor, for thermal management.

The carrier mobility is a major factor in determining the speed of electronic devices. As the dimensions of nanoelectronic circuits continue to shrink, it is important that the carrier mobility does not deteriorate and, if possible, improves. A generic nanostructure such as nanowire (NW) represents a convenient system to understand the effects of low dimensionality on the carrier drift mobility. One can also look at NW as an ultimately scaled transistor channel. Early optimism about enhancement of the electron mobility limited by impurity scattering in NWs[1] quickly turned into more pessimistic outlook when it was shown that quantum confinement of electrons increased the electron−phonon deformation potential scattering in NWs with small diameters.[2] The calculations of Lee and Vassell[2] assumed that the electrons are confined within NW while acoustic phonons are bulklike and extend beyond the NW boundaries. More bad news for carrier mobility followed when it became clear that spatial confinement of acoustic phonons in thin freestanding NW leads to further increase in the confined electron−confined phonon scattering rates.[3] Despite these not very optimistic prospects, the search for the nanostructures where the carrier mobility values can be preserved or even improved continues[4] owing to the extremely high technological pay-off if successful.

In this Letter we demonstrate theoretically that the carrier mobility can be enhanced in a Si NW with a barrier shell made of the acoustically hard material such as diamond (the acoustic hardness is characterized by the product of the mass density and the sound velocity). This result overturns conventional believe that the phonon confinement effects are always detrimental to the carrier mobility. Potentially, it may also impact the design of the ultimately scaled CMOS and beyond-CMOS electronic devices, e.g., carbon-based or heterogeneous Si−carbon nanodevices.

Our results are obtained for NWs, which are realistic from the technological point of view. Indeed, in order for phonon confinement effects to take place, the NW diameter D has to be of the order of the thermal phonon wavelength $\lambda_0 = hc_l/(k_BT)$ (h is Planck's constant, k_B is the Boltzmann constant, T is absolute temperature, c_l and c_t are the longitudinal and transverse sound velocities, respectively). The values of c_l and c_t for the considered materials are listed in Table 1. For Si at room temperature $\lambda_0 = 1.35$ nm. High-quality crystalline Si NWs with diameters as small as $D = 2$ nm have already been fabricated.[5−9] The fabricated NWs are either freestanding[6−9] or coated with SiO_2.[5] The diamond barrier shells for Si NWs, which are required for achieving the mobility enhancement, are also quite feasible. Dennig et al.[10] demonstrated that the single-crystal diamond can be grown around thin Si NWs using plasma-enhanced chemical vapor deposition (CVD). Zhang et al.[11] employed the hot-filament CVD method to deposit multiple graphitic carbon layers around thin Si NWs. As a result, Si NWs appeared inside a multiwall carbon nanotube. Subsequent hydrogen plasma post-treatment of the multiwalled carbon nanotube was shown to result in the formation of diamond shells.[12] In our calculations, diamond is used as an example of the acoustically hard material, which is compatible with Si, and can provide an extra advantage of high thermal conductivity for thermal management.

* Corresponding author: balandin@ee.ucr.edu.

10.1021/nl061554o CCC: $33.50
Published on Web 10/19/2006

Table 1. Longitudinal and Transverse Sound Velocities and Mass Density for Silicon and Coating Materials Considered Here

	c_l (m/s)	c_t (m/s)	ρ (g/cm^3)
Si	8430	5840	2.33
diamond	17500	12800	3.512
SiO_2	5900	3750	2.20

In the GaAs-based high-electron mobility transistors and Si/high-K-dielectric devices, the interface traps present a substantial mobility-limiting factor. At the same time, one can expect a cleaner interface between Si NW and the diamond shell, particularly with further advancement in the NW fabrication technology.[7−9] Recently, it has been experimentally demonstrated that no additional leakage currents or charge trapping were present in the thin Si-on-diamond devices as compared to Si-on-SiO_2 devices.[13] For this reason we focused our analysis on the other dominant mobility limiting mechanisms such as the phonon and charged impurity scattering.

In Si NWs with small diameters ($D < 5-10$ nm) spatial confinement affects both the charge carriers and phonons. Bulk Si has indirect band gap with six equivalent conduction band minima. On the other hand, it was recently shown that Si NWs with $D = 3-10$ nm grow along the $\langle 110 \rangle$ axis[9] and exhibit a direct band gap at the Γ point of the Brillouin zone.[14] The latter simplifies theoretical treatment of Si NWs. The main mechanism that limits the low-field carrier mobility in Si NWs near room temperature is the carrier scattering on lattice vibrations, i.e., acoustic phonons. For NWs with diameters of tens of nanometers and temperatures of hundreds of kelvin, phonon confinement effects can be safely neglected and the scattering rate calculation can assume the "bulklike" phonons. The term bulklike phonon implies that NW is embedded in a hypothetic medium, impenetrable for the charge carriers, with the elastic parameters equal to those of NW. However, since we consider NWs with diameters of only a few nanometers, the phonon confinement effects are strong and have to be taken into account.[4]

Assuming that only the lowest electron subband in Si NW is populated, the electron momentum relaxation rate due to the acoustic phonons can be calculated as

$$\tau_{\mathrm{ph}}^{-1}(k_z) = \frac{2\pi}{\hbar} E_a^2 \sum_{\mathbf{q}} |\langle \nabla \cdot \mathbf{u}_{\mathbf{q}} \rangle|^2 \frac{q_z}{k_z} [(N_{\mathbf{q}} + 1)\delta(\epsilon_{k_z - q_z} + \hbar\omega_{\mathbf{q}} - \epsilon_{k_z}) + N_{-\mathbf{q}}\delta(\epsilon_{k_z - q_z} - \hbar\omega_{-\mathbf{q}} - \epsilon_{k_z})] \quad (1)$$

Here, ϵ_{k_z} is the electron energy,[15] $E_a = 12$ eV[16] is the acoustic deformation potential, $\omega_{\mathbf{q}}$ is the phonon frequency, $N_{\mathbf{q}}$ is the phonon occupation number given by the Bose−Einstein distribution, and $\mathbf{u}_{\mathbf{q}}$ is the phonon displacement vector normalized as $\int_V \rho(\mathbf{r})|\mathbf{u}_{\mathbf{q}}|^2 \, d\mathbf{r} = \hbar/(2\omega_{\mathbf{q}})$, where $\rho(\mathbf{r})$ is the mass density (see Table 1) and V is the volume of the system. The divergence of the displacement vector in eq 1 is averaged in the direction perpendicular to the NW axis using the ground state electron density. Note that eq 1 is valid for scattering on the bulklike phonons as well as for scattering on confined phonons. In the case of confined phonons, the displacement vector has been found as a solution of the equation of motion.[17] We employed the boundary conditions that require the continuity of the displacement vector and the stress tensor across the Si−diamond interface as well as finiteness of the displacement vector at the NW axis and vanishing of the stress tensor at the outer surface. In the case of the electron scattering on confined phonons, the phonon wave vector $\mathbf{q}$ is quantized in the lateral direction; thus the summation in eq 1 is carried out over q_z and the discrete spectrum of phonon frequencies ω.

Realistic NWs always contain some charged impurities originating from the doping or defects. Charged impurities introduce another scattering mechanism, which has to be accounted for in order to calculate the electron mobility. The electron momentum relaxation rate for the ionized impurity scattering can be calculated as[18]

$$\tau_{\mathrm{imp}}^{-1}(k_z) = \frac{2\pi m N_I R_1^2}{\hbar^3 k_z} \left(\frac{Ze^2}{2\pi\epsilon_0\epsilon} \right)^2 [\ln(k_z R_1)]^2 \quad (2)$$

where N_I and $Z = 1$ are the concentration and charge of the impurities, m is the electron effective mass,[15] and R_1 and $\epsilon = 11.7$ are the NW radius and dielectric constant,[19] respectively. For our calculations we chose $N_I = 5 \times 10^{19}$ cm^{-3} (0.1 atomic %), which is the upper limit of the reported impurity concentrations in Si NWs. The total relaxation rate, $\tau^{-1} = \tau_{\mathrm{ph}}^{-1} + \tau_{\mathrm{imp}}^{-1}$, is used to calculate the low-field drift electron mobility in NWs as

$$\mu = -2\frac{e}{m}\left\{ \int_0^\infty \epsilon^{1/2} \frac{\partial f_0}{\partial \epsilon} \tau(\epsilon) \, d\epsilon / \int_0^\infty \epsilon^{-1/2} f_0(\epsilon) \, d\epsilon \right\} \quad (3)$$

where $f_0(\epsilon)$ is the electron occupation number given by the Fermi−Dirac distribution. In the case of nondegenerate carrier statistics, $f_0(\epsilon)$ is given by a Maxwellian distribution.

To separate the effects of the electron and phonon confinement on electron mobility in Si NWs, we first calculate electron mobility as a function of the NW diameter using the bulklike phonons. The room-temperature electron mobility as a function of the NW diameter (assuming that the electrons are confined while the phonons are not) is shown in Figure 1. One can see that the electron mobility decreases with decreasing NW diameter proportionally to D^2. This result is expected and in line with the prediction made for NWs made of another material system such as GaAs.[2] The increase of electron mobility with the NW diameter stops as higher electron subbands start to participate in the scattering process. For the considered Si NWs, the distance between the two lowest electron subbands decreases from 326 to 52 meV as D increases from 4 to 10 nm. For 10-nm Si NWs, the subband separation is only two times the thermal energy $k_B T$ at room temperature, which suggests the appearance of inter-subband transitions for NWs with diameter larger than 10 nm. For this reason, the part of the mobility dependence, which corresponds to the larger diameter NWs, where the single-subband treatment is not valid, is shown with the dashed curve.

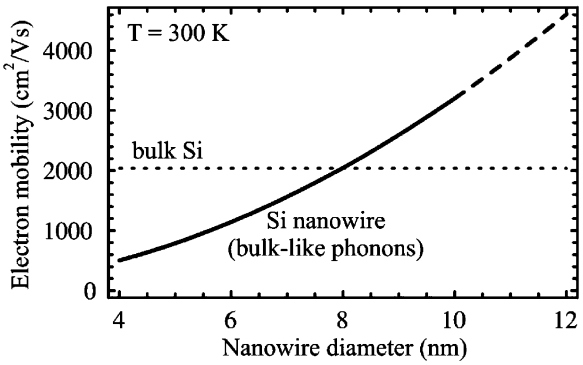

Figure 1. Size dependence of low-field electron mobility in silicon nanowires.

The dotted straight line in Figure 1 shows the result of our calculation for the "infinitely thick" Si NWs. The obtained value is about 25% higher than the measured electron mobility in bulk Si. The discrepancy is due to the fact that in our model we took into account that narrow Si NWs have a direct band gap at the Γ point[14] and as the NW diameter increases in the infinitely thick Si NW limit this assumption becomes invalid. One can see from Figure 1 that the electron mobility for Si NWs thicker than 8 nm is higher than that for bulk Si. Thus, in Si NWs with confined electron (but bulklike phonons) there exist a narrow range of NW diameters where mobility is enhanced as compared to bulk Si. This finding is in agreement with the available experimental data. The measurements reported for 10-nm p-type Si NWs[20] gave a mobility of 560 $cm^2/(V\ s)$, which is larger than the intrinsic hole mobility in bulk Si (450 $cm^2/(V\ s)$). Similarly, for other material systems, the measured mobility for 10-nm n-type GaN NWs[21] is in the range 150−650 $cm^2/(V\ s)$, which is comparable to or larger than the intrinsic electron mobility in bulk GaN (440 $cm^2/(V\ s)$). On the other hand, in wider 20-nm p-type Ge NWs[22] and n-type Si NWs,[23] the measured mobility is 3 to 9 times less than that for the corresponding bulk materials. For thicker 40-nm n-type CdS and ZnO NWs, the measured mobility is 11 to 22 times less than that for corresponding bulk materials.[24] These experimental data suggest that the inter-subband scattering in NWs with $D > 10$ nm significantly reduces the carrier mobility.

After the effect of the electron confinement (quantization) on the carrier mobility is clarified, we can focus on the effect of the acoustic phonon confinement in NWs with the acoustically hard barriers. Figure 2 shows the evolution of the spectrum of confined phonons in the diamond-coated 4-nm Si NW with increasing thickness of the diamond coating. The size of the circles for each phonon mode is proportional to the average deformation potential (divergence of the displacement vector) that enters eq 1. Note that our calculation took into account phonons with higher q_z and ω; however, the contribution to the scattering rate from the higher-frequency modes is negligible in comparison with the contribution from the modes shown in Figure 2. The energy conservation law given by the delta functions in eq 1 and the multiplier q_z/k_z lead to the fact that phonons with $q_z \approx 2k_z$ give the main contribution to the scattering of electrons with the wave vector k_z ($q_z = 2k_z$ corresponds to the electron backscattering). To estimate the scattering rate from dependences shown in Figure 2, one has to perform the summation of the amplitudes at $q_z \approx 2k_z$ (given by the circle sizes) squared and weighted with the corresponding phonon occupation number.

As seen in Figure 2, the dispersion of the lowest "true acoustic" phonon mode is linear in the region of small q_z. The velocity of this true acoustic mode increases with the thickness of diamond barrier shell (i.e., coating) and changes from the value of the longitudinal sound velocity in Si to the value of the longitudinal sound velocity in diamond (see Table 1). At the same time, the contribution of this mode to electron scattering (indicated by the circle sizes) strongly decreases with the thickness of the diamond coating. For a relatively thick diamond barrier, the true acoustic mode does not participate in the electron scattering. This is analogous to the case of NWs with the so-called *clamped* surface boundaries (see the last panel in Figure 2), characterized by zero displacement at the surface. The comparison of all panels in Figure 2 clearly shows that the scattering amplitudes become less like for the free-standing NW and more like for the clamped NW as the thickness of the diamond barrier shell increases. The phonon spectrum modification shown in Figure 2 implies that the scattering rate (and therefore the electron mobility) of Si NWs coated with diamond varies between two limiting cases, which correspond to the free-surface (i.e., free-standing) and clamped-surface NWs.

Figure 3 shows the electron mobility μ calculated according to eq 3 with the actual acoustic phonon spectrum found for the 4-nm Si NW coated with diamond. The μ values are between the limits corresponding to the free-standing and clamped Si NWs for all considered temperatures. As expected, the case of bulklike phonons also results in the electron mobility, which falls between the same limits. As the thickness of diamond barrier shell increases, the mobility approaches the limit of the clamped NW. This result is unexpected and very important. Previously, the clamped-surface boundaries were considered to be impractical, i.e., unachievable in any sort of realistic structures,[3] and all other considered boundaries were shown to lead to increased confined electron−confined phonon scattering.[25−27] Our calculations have demonstrated that even a thin barrier made of diamond modifies the phonon spectrum in Si NWs to such a degree that it becomes similar to that in the clamped-surface NWs. Moreover, the confined electron−confined phonon scattering rates in diamond-coated Si NWs decrease significantly, leading to the strong mobility enhancement in comparison with the free-standing NWs (see Figures 3 and 4). To understand the physics underlying this phenomenon, one has to recall (see Figure 2) that for the clamped NW the number of phonons participating in the scattering is less and the amplitude of the scattering is lower than that for the free-standing NW.

One can also see from Figure 3 that at low temperatures the mobility is limited by impurities and proportional to $T^{1/2}$. At high temperatures the mobility is limited by phonons and proportional to $T^{-1/2}$. The change of the temperature

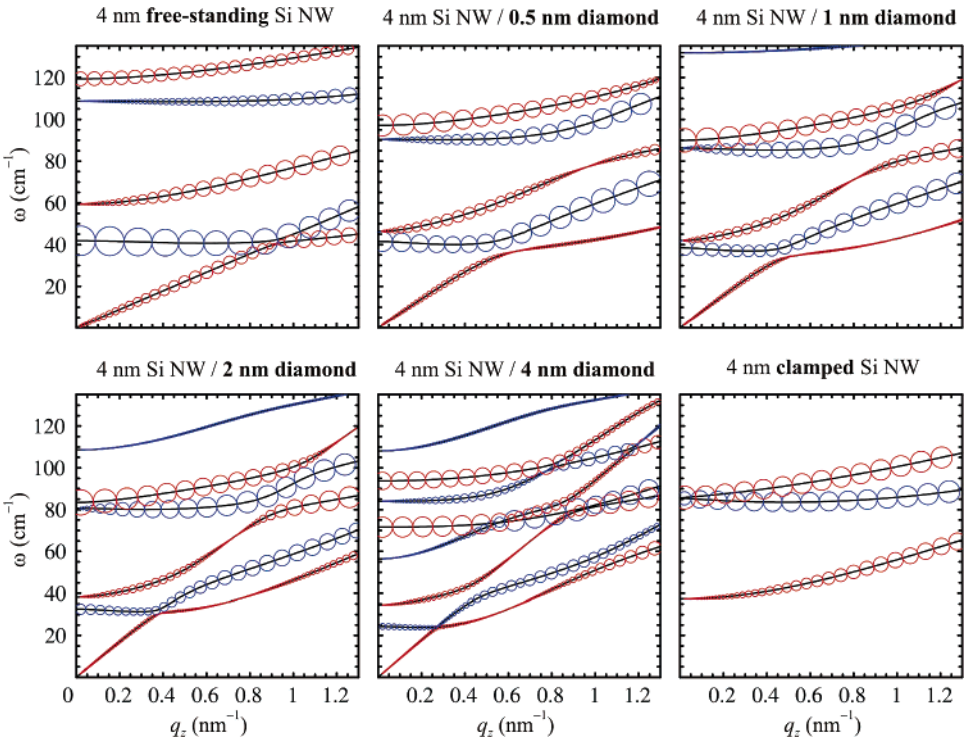

Figure 2. Phonon dispersion in free-standing, coated with diamond, and clamped 4-nm silicon nanowires. The size of circles is proportional to the average divergence of the corresponding displacement vector.

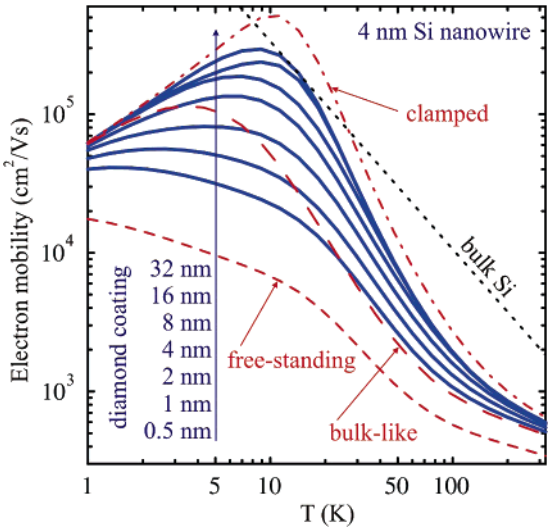

Figure 3. Low-field electron mobility as a function of temperature for 4-nm silicon nanowires with and without diamond coating. Dotted line shows electron mobility for pure bulk silicon.

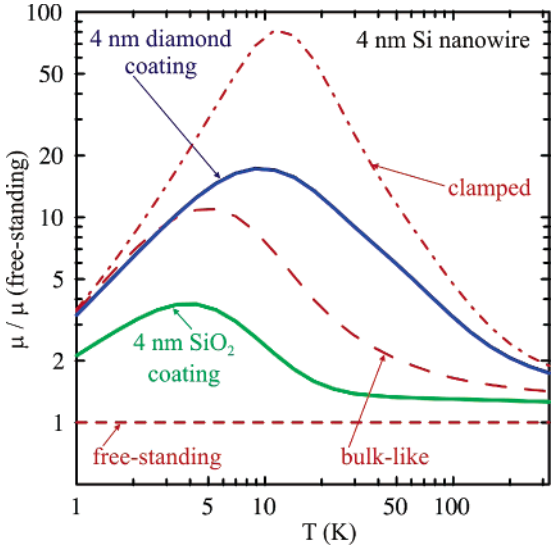

Figure 4. Enhancement of low-field electron mobility for coated 4-nm silicon nanowires in comparison with the free-standing nanowire.

dependence of mobility from the $T^{3/2}$ ($T^{-3/2}$) in bulk nonpolar semiconductors to the $T^{1/2}$ ($T^{-1/2}$) dependence in Si NWs reflects the change in the electron density of states as one goes from bulk to NWs. Another observation is that the electron−phonon scattering rate in the free-standing NW is so strong that it limits the electron mobility even at low temperatures. On the other hand, the electron−phonon scattering in diamond-coated Si NWs with 0.1 atomic % of impurities is so weak that the electron mobility becomes comparable with the mobility of pure bulk Si. At room temperature, even 0.5-nm-thick diamond coating results in the electron mobility, which is higher than that in the case of bulklike phonons. If the barrier shell (coating) material is softer than Si, the electron mobility is always lower than in the case of bulklike phonons. The latter is the case for practically important SiO_2 coating. Results presented in Figure 4 suggest that the electron mobility enhancement due to diamond coating can be as high as *2* orders of magnitude at about 10 K and about a *factor of 2* at room temperature. Since diamond materials are excellent heat conductors (even in microcrystalline form[28]), the electron mobility enhancement is accompanied by an extra benefit of improved thermal management.

In conclusion, we have proposed a method for the enhancement of the carrier mobility in Si NWs. Our detailed calculations elucidated the physical mechanisms, which lead to a strong mobility increase in a wide temperature range, including room temperature. The proposed technologically feasible approach is based on coating of NWs with an acoustically hard material such as diamond. Our work revises the long-standing belief that the spatial confinement induced modification of the phonon spectrum is always detrimental to the carrier mobility.

Acknowledgment. This work has been supported, in part, by MARCO Focus Center on Functional Engineered Nano Architectonics (FENA), DMEA-DARPA Center for Nanoscience Innovation for Defense (CNID), and NSF Nanoscale Exploratory Award (NER) to A.A.B.

References

(1) Sakaki, H. *Jpn. J. Appl. Phys.* **1980**, *19*, L735.
(2) Lee J. ; Vassell, M. O. *J. Phys. C: Solid State Phys.* **1984**, *17*, 2525.
(3) Yu, S. G.; Kim, K. W.; Stroscio, M. A.; Iafrate, G. J.; Ballato, A. *J. Appl. Phys.* **1996**, *80*, 2815.
(4) Fonoberov, V. A.; Balandin, A. A. *Nano Lett.* **2005**, *5*, 1920. Pokatilov, E. P.; Nika, D. L.; Balandin, A. A. *Superlatt. Microstruct.* **2005**, *38*, 168. Pokatilov, E. P., Nika, D. L., Balandin, A. A. *Phys. Rev. B* **2005**, *72*, 113311.
(5) Liu, H. I.; Biegelsen, D. K.; Ponce, F. A.; Johnson, N. M.; Pease, R. F. W. *Appl. Phys. Lett.* **1994**, *64*, 1383.
(6) Holmes, J. D.; Johnston, K. P.; Doty, R. C.; Korgel, B. A. *Science* **2000**, *287*, 1471.
(7) Cui, Y.; Lauhon, L. J.; Gudiksen, M. S.; Wang, J. F.; Lieber, C. M. *Appl. Phys. Lett.* **2001**, *78*, 2214.
(8) Huang, Y.; Duan, X.; Cui, Y.; Lauhon, L. J.; Kim, K.-H.; Lieber, C. M. *Science* **2001**, *294*, 1313.
(9) Wu, Y.; Cui, Y.; Huynh, L.; Barrelet, C. J.; Bell, D. C.; Lieber, C. M. *Nano Lett.* **2004**, *4*, 433.
(10) Dennig, P. A.; Liu, H. I.; Stevenson, D. A.; Pease, R. F. W. *Appl. Phys. Lett.* **1995**, *67*, 909.
(11) Zhang, Y. F.; Tang, Y. H.; Zhang, Y.; Lee, C. S.; Bello, I.; Lee, S. T. *Chem. Phys. Lett.* **2000**, *330*, 48.
(12) Sun, L. T.; Gong, J. L.; Zhu, Z. Y.; Zhu, D. Z.; Wang, Z. X.; Zhang, W.; Hu, J. G.; Li, Q. T. *Diamond & Related Materials* **2005**, *14*, 749.
(13) Aleksov, A.; Gobien, J. M.; Li, X.; Prater, J. T.; Sitar, Z. *Diamond Relat. Mater.* **2006**, *15*, 248.
(14) Zhao, X.; Wei, C. M.; Yang, L.; Chou, M. Y. *Phys. Rev. Lett.* **2004**, *92*, 236805. Zheng, Y.; Rivas, C.; Lake, R.; Alam, K.; Boykin, T. B.; Klimeck, G. *IEEE Trans. Electron Devices* **2005**, *52*, 1097.
(15) Inverse electron effective mass for thin Si nanowires was calculated as the directional average of inverse electron effective masses for bulk Si, which resulted in $m = 0.26m_0$.
(16) Kotlyar, R.; Obradovic, B.; Matagne, P.; Stettler, M.; Giles, M. D. *Appl. Phys. Lett.* **2004**, *84*, 5270.
(17) Balandin, A. A.; Fonoberov, V. A. *J. Biomed. Nanotechnol.* **2005**, *1*, 90. Fonoberov, V. A.; Balandin, A. A. *Phys. Status Solidi B* **2004**, *241*, R67.
(18) Lee, J.; Spector, H. N. *J. Appl. Phys.* **1983**, *54*, 3921.
(19) The screening of charged impurities by electrons is not taken into account; the screening reduces electron-impurity scattering and increases low-temperature electron mobility.
(20) Cui, Y.; Zhong, Z. H.; Wang, D.; Wang, W. U.; Lieber, C. M. *Nano Lett.* **2003**, *3*, 149.
(21) Huang, Y.; Duan, X. F.; Cui, Y.; Lieber, C. M. *Nano Lett.* **2002**, *2*, 101.
(22) Wang, D. W.; Wang, Q.; Javey, A.; Tu, R.; Daia, H. J.; Kim, H. S.; McIntyre, P. C.; Krishnamohan, T.; Saraswat, K. C. *Appl. Phys. Lett.* **2003**, *83*, 2432.
(23) Zheng, G. F.; Lu, W.; Jin, S.; Lieber, C. M. *Adv. Mater.* **2004**, *16*, 1890.
(24) Zhang, Z. Y.; Jin, C. H.; Liang, X. L.; Chen, Q.; Peng, L.-M. *Appl. Phys. Lett.* **2006**, *88*, 073102.
(25) Yu, S. G.; Kim, K. W.; Stroscio, M. A.; Iafrate, G. J. *Phys. Rev. B* **1995**, *51*, 4695.
(26) Nishiguchi, N. *Phys. Rev. B* **1996**, *54*, 1494.
(27) Svizhenko, A.; Balandin, A.; Bandyopadhyay, S.; Stroscio, M. A. *Phys. Rev. B* **1998**, *57*, 4687.
(28) Liu, W. L.; Shamsa, M.; Calizo, I.; Balandin, A. A.; Ralchenko, V.; Popovich, A.; Saveliev, A. Thermal conduction in nanocrystalline diamond films: Effects of the grain boundary scattering and nitrogen doping. *Appl. Phys. Lett.*, in press.

NL061554O